Thermochimica Acta 512 (2011) 5–12

Contents lists available at ScienceDirect

Thermochimica Acta

journal homepage: www.elsevier.com/locate/tca

Thermal analysis of monument patina containing hydrated calcium oxalates

J.L. Perez-Rodriguez[a], A. Duran[a,*], M.A. Centeno[a], J.M. Martinez-Blanes[a], M.D. Robador[b,1]

[a] Materials Science Institute of Seville (CSIC-University of Seville), Americo Vespucio 49, 41092 Seville, Spain
[b] Technical Architecture Faculty (University of Seville), Reina Mercedes 4, 41002 Seville, Spain

ARTICLE INFO

Article history:
Received 21 May 2010
Received in revised form 2 August 2010
Accepted 18 August 2010
Available online 21 August 2010

Keywords:
Patina
Hydrated calcium oxalates
DTA/TG
High-temperature XRD
Mass spectrometry
DRIFTS
Cultural heritage
Romanesque Church of Torme

ABSTRACT

This work describes the thermal transformation of patina samples formed on the surface of dolomitic rocks used to build the Romanesque Torme's Church (Burgos, Spain). Analyses were performed using a combination of high-temperature XRD, simultaneous TG/DTA and gas mass spectrometry. The XRD analysis revealed the presence of hydrated calcium oxalates. The following three steps were proposed for the thermal transformation of the raw material: dehydration of weddellite/whewellite to form calcium oxalate, transformation of calcium oxalate to calcium carbonate, and formation of calcium oxide produced via decomposition of the calcite. DTA/TG and mass spectrometry analyses confirmed this mechanism. In addition, a high proportion of organic compounds was detected and was possibly formed via degradation of products applied for the building's conservation by the action of microorganisms attack. Mass spectrometry analysis revealed CO (and CO_2) gas evolved during the transformation of CaC_2O_4 to $CaCO_3$. The CO_2 gas also appears at 765 °C due to the decomposition of calcium carbonate, and it appears over a large range of temperatures due to the decomposition of organic compounds. The TG analyses performed in a CO_2 atmosphere were used to determine the percentages of Ca and Mg contained in dolomite, and the calcium carbonate formed by oxalate decomposition. DRIFTS and mass spectrometry results revealed the presence of several aliphatic and/or aromatic compounds containing C=O groups.

1. Introduction

Several literature reports focus on the decay and preservation of building materials. Some authors have suggested that the formation of crusts and patinas on buildings includes a biological component that relies upon oxalic acid secreted by microorganisms in the calcareous rocks and mortars of buildings (e.g., algae, lichens, fungi, etc.) [1–7]. Many other authors maintain that patina formation is of artificial/anthropogenic origin via past conservation/restoration treatments and via degradation of the products applied by the action of microorganisms [8,9]. Oxalates have been identified on the surface of monuments, art objects, frescos and primitive paintings [10–13]; and such compounds have been identified as responsible for these objects' decay and/or degradation.

The type of oxalates formed in these processes depends on the type of material involved. The oxalic acid attacks calcium carbonate ($CaCO_3$) and precipitates as calcium oxalate, an insoluble calcium salt [5,14–16]. Calcium oxalate films are very stable and are hardly affected by atmospheric pollution [15]. In some cases, calcium oxalate occurs as the monohydrate salt, whewellite ($CaC_2O_4{\cdot}H_2O$), and the dihydrate salt, weddellite ($CaC_2O_4{\cdot}2H_2O$) [5,6,16]. The formation of the mineral glushinskite ($MgC_2O_4{\cdot}H_2O$) occurs through fungal interaction with dolomitic rock and seawater substrates [17].

Thermal treatment has been used as a method for characterising oxalates [18–21]. Oxalates are frequently used for the calibration of thermal analysis equipment. Several authors have reported three mass-loss steps during thermogravimetric studies of dihydrated calcium oxalate. In the first mass-loss step, water is evolved; in the second and third steps, CO and CO_2 are evolved, respectively [20,22,23]. Frost and Weier [18,21] used thermogravimetric and mass spectrometry analyses to identify the presence of carbon dioxide in the second and third mass-loss steps.

The Church of Torme is a Romanesque-style building from the 12th century. It has a marvellous apse, and it is situated in a forested area in the northern of the Burgos province. Dolomite is the main component of the building's rock, and a patina composed of hydrated calcium oxalates has been detected [24].

The main objective of this work was to study the oxalate patina formed on the dolomite rocks of Torme's Church by using thermal analysis together with other complementary techniques. The processes occurring during thermal decomposition of the patina are also discussed. During this decomposition, oxalates and other organic compounds formed by bio-deterioration processes are considered.

* Corresponding author. Tel.: +34 954489576; fax: +34 954460665.
E-mail address: adrian@icmse.csic.es (A. Duran).
[1] Tel.: +34 954556611; fax: +34 954556691.

0040-6031/$ – see front matter © 2010 Elsevier B.V. All rights reserved.
doi:10.1016/j.tca.2010.08.015

2. Experimental

2.1. Sampling

Ten samples were collected from the external walls of the Romanesque Church of Torme. Each was collected from different zones of the building; four samples were taken from the apse, and the others were taken from other facades on the northern side of the structure (all of them in different locations). It is possible that differences could be found between the results obtained due to the heterogeneity of the samples.

2.2. Methods

Thermal analysis was performed using a simultaneous TG/DTA (thermogravimetry/differential thermal analysis) instrument (STD Q600, TA Instruments). Measurements were conducted under flowing air, N_2 or CO_2; and the samples were heated at a linear heating rate of 10 °C min^{-1}.

X-ray diffraction (XRD) analyses were performed using a Panalytical diffractometer X'Pert Pro MPD. The measurements used Cu Kα radiation (40 kV, 40 mA) covering a 2θ range between 10 and 60°. The detector was an X'Cellerator detector with an angular aperture of 2.18° (2θ) and a step size of 0.016° (2θ). Heating experiments were carried out in a HTK 1200 high-temperature chamber (Anton Paar). Experiments were performed under flowing air and at temperatures ranging from room temperature to 1000 °C with a heating rate of 10 °C min^{-1}. XRD diagrams of the samples were collected every 50 °C.

Temperature-programmed oxidation and desorption of the patina and a commercial $C_2O_4{\cdot}H_2O$ sample (provided by FLUKA) were followed by mass spectrometry using a Balzers Thermostar benchtop mass spectrometer. The samples were placed among quartz wool in a continuous-flow, U-shape quartz reactor. A 50 ml min^{-1} flow of synthetic air or helium was passed through the reactor, and the temperature was increased to 800 °C at 10 °C min^{-1}.

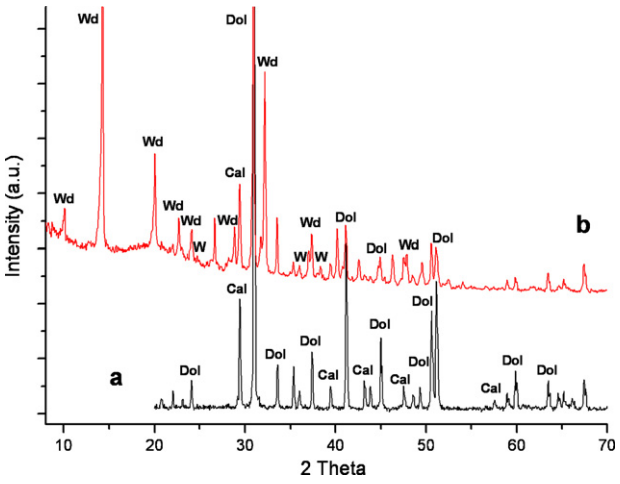

Fig. 1. XRD patterns corresponding to (a) the rock substrate of Torme's Church; (b) the patina covering the walls of the Church [Dol = dolomite, Cal = calcite, Wd = weddellite, W = whewellite].

A scanning electron microscope (model HITACHI S-4800) was used. An energy dispersive X-ray analyser (EDX) coupled to the SEM, was employed for elemental analysis. The samples were coated with a gold film before the SEM/EDX study (Mα and Lα lines of gold at 2.12 and 9.71 keV, respectively, are observed in some of the EDX spectra).

The Fourier-transform infrared (FT-IR) absorbance measurements were performed at wavenumbers ranging from 400 to 4000 cm^{-1} and were performed using a Nicolet 510 spectrometer (Source: Globar, Detector: DTGS). The samples in powder form were mixed with KBr.

Diffuse-reflectance infrared Fourier-transform spectroscopy (DRIFTS) measurements were collected using a Thermo Nicolet Nexus infrared spectrometer with KBr optics, a Global source and a MCT/B detector working at the temperature of liquid nitrogen. Samples were placed without any treatment, such as crashing or dilution, on a diffuse-reflectance accessory (Spectra Tech), and the

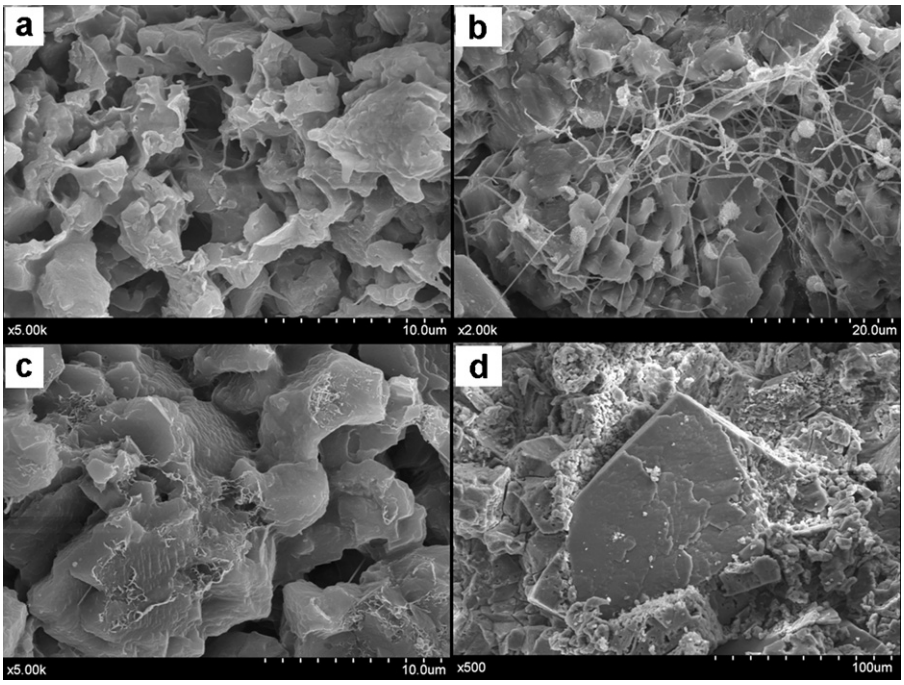

Fig. 2. SEM images of (a) dolomite particles in the rock; (b) microorganisms on the Church's rock; (c) product applied covering the rock; and (d) calcite particles in the rock.

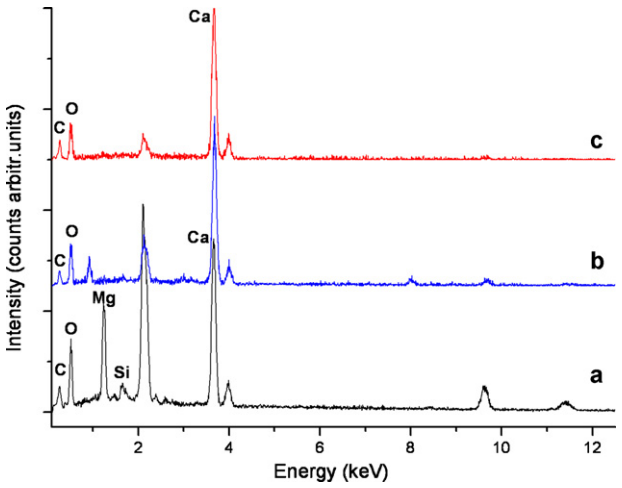

Fig. 3. EDX analyses of (a) the Church's rock substrate; (b) the calcite grains composing the rock; and (c) the patina covering the walls of the Church.

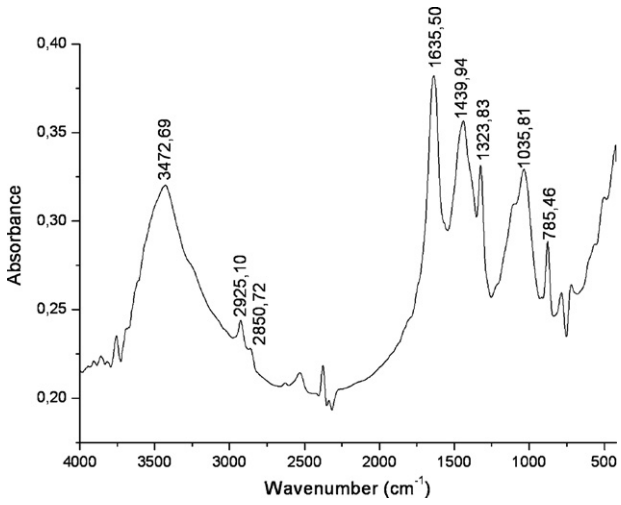

Fig. 4. Infrared spectra corresponding to the patina on the Church.

spectra (64 scans, 4 cm^{-1} resolution) were collected at room temperature under atmospheric conditions.

3. Results and discussion

3.1. Rock substrate of the Torme's Church

X-ray diffraction analyses of the rock substrate indicated the presence of dolomite [$CaMg(CO_3)_2$]. In addition, small amounts of calcite were also detected (Fig. 1a). The morphology of the rock was observed using SEM (Fig. 2). The dolomite particles exhibited holes, and some particles had undergone degradation (break-down) processes (Fig. 2a). Some biological activity was also observed (Fig. 2b), and some organic products were also on the rock's surface (Fig. 2c). Elemental chemical analysis performed using EDX showed the presence of calcium, magnesium and silicon (Fig. 3a). Particles larger than the dolomite were scarce (Fig. 2d) and were constituted by calcite. The composition was confirmed by EDX analyses, which detected only calcium (Fig. 3b). The results were very similar for all samples collected from the historical building.

3.2. Oxalate patina of the Torme's Church

3.2.1. XRD, FT-IR and SEM-EDS studies at room temperature

The patina was very uniform along the entire monument and had a yellow-reddish colour with variations of colour depending on the location. Regarding the identification of the compounds forming the patina, almost identical qualitative results were obtained for all of the samples analysed. The room-temperature XRD diagram for samples from this superficial layer covering the walls of the Church showed the presence of oxalate compounds (weddellite and a minor proportion of whewellite), dolomite and calcite (Fig. 1b). The FT-infrared spectra exhibited bands at 1635, 1323 and 785 cm^{-1} (Fig. 4), which were each assigned to oxalate compounds [25]. The two prominent bands at 1635 and 1323 cm^{-1} are related to water vibrations and OCO-deformation (asymmetric and symmetric stretching vibrations of the oxalate's carboxylate group), respectively [26–28]. Bands ascribed to carbonates (1439 cm^{-1}) and silicates (1035 cm^{-1}) were also detected by FT-IR, but these signals likely arose from the carbonate compounds and the silicates (indicated by the presence of silicon in the EDX elemental analysis) detected in the rock substrate. Absorbances at 2925 and 2850 cm^{-1} were also observed and were assigned to aliphatic C–H stretching bands, which correspond to some types of organic compounds. FT-IR experiments performed on a commercial sample of standard whewellite did not exhibit absorbance bands associated with organic compounds, carbonates and/or silicates (data not shown).

Only calcium was detected in the EDX study performed on the superficial zones of the samples taken from the Church's walls (Fig. 3c), where the oxalate compounds are found (Fig. 5). SEM images revealed mineral neoformation on the rock substrate, and XRD analyses indicated that this mineral material corresponded mainly to weddellite. A concentric structure, reflecting crystal growth around a nucleus, is shown in Fig. 5a and c. Small particles of hydrated calcium oxalates were also observed (Fig. 5a–c). Bipyramidal prisms of weddellite were observed in the samples studied, although cubes of whewellite were also present in small proportions (Fig. 5d).

The uniformity of the patina along whole the external of the building, the FT-IR detection of organic compounds (Fig. 4), the SEM observation of microorganisms (Fig. 2b) and the observation of some organic product applied over the stone (Fig. 2c) indicate that oxalates were very possibly formed via microbial degradation of organic products that were applied during protection/restoration of the building. The formation of calcium oxalates on the surface of stones is associated with the degradation of past surface treatments, a process that has been discussed in the literature [29,30]. In the agglomerates of hydrated calcium oxalate, there may also be embedded biological components (e.g., polysaccharides or proteins). Rich biominerals formed highly ordered and packed crystal encrustations on organic compounds [17].

In this work, weddellite was the main oxalate component and was accompanied by a small percentage of whewellite. Both occurred simultaneously in the growth environment. Coexistence of the two mineral species was attributed to biological activity [31] and depended on a variety of factors including the pH, temperature, solubility of the oxalates and diagenetic crystallisation [24,32,33].

The source of calcium was dolomite, which is also composed of magnesium. The mineral glushinskite ($MgC_2O_4{\cdot}2H_2O$) was not found in the surface layer of the studied building. All of the EDX and XRD analyses showed that the samples were composed of a Ca-bearing mineral. Kolo and Claeys [17] illustrated a sequence of possible uptake-expulsion processes for Ca^{2+} and Mg^{2+} by fungi in a dolomitic substrate. Since the Mg-oxalates have a much higher solubility than Ca-oxalates [34], fungi first neutralise the Ca^{2+} through Ca uptake. Calcium is excreted outside of the cell walls and is removed from the biological growth environment in the form of insoluble Ca-oxalates [17,35]. The high Mg concentrations necessary for glushinskite precipitation are only possible in a localised

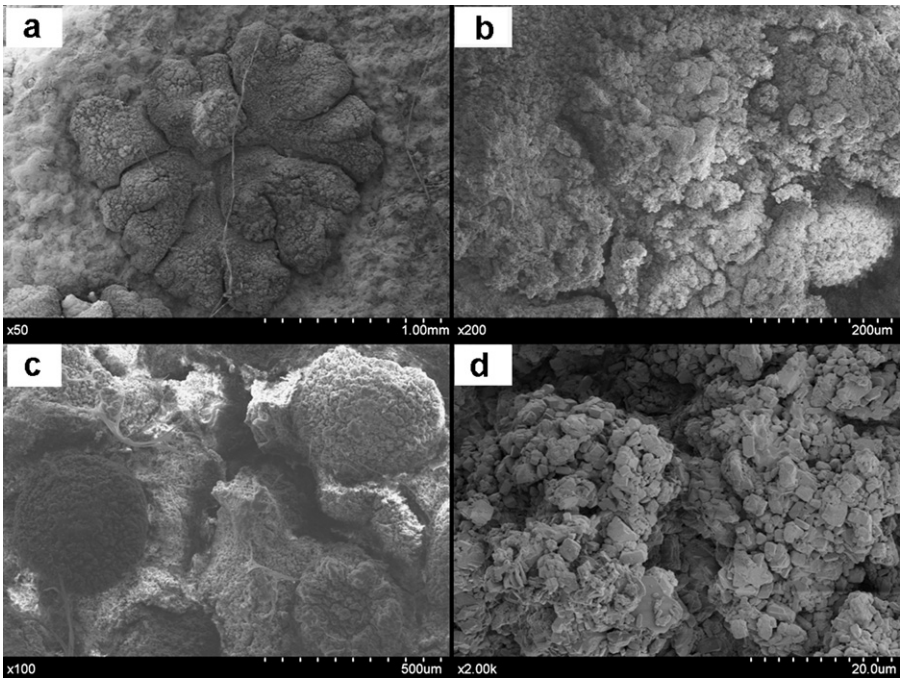

Fig. 5. SEM images of the Church's patina. (a and b) Neoformation of weddellite and whewellite on the substrate; (c) crystals growth mechanism around a nucleus; and (d) morphology of the crystals (i.e., bipyramidal prisms of weddellite and cubes of whewellite).

environment. These factors could explain the lack of Mg-oxalate in this study's samples.

3.2.2. Thermal studies (XRD, TG, DTA, mass spectrometry, DRIFTS)

To study the thermal transformations of the patina's compounds, the samples were heated and examined using XRD. At room temperature, weddellite and dolomite were detected along with small amounts of calcite and whewellite (Figs. 1b and 6a). Some changes in the XRD diagrams occurred during the heating process. Between 100 and 200 °C, the transformation of hydrated calcium oxalates (i.e., weddellite and whewellite) to calcium oxalate was detected (Fig. 6b). At 400 °C, the $CaCO_3$ content increased due to the formation of calcite via decomposition of CaC_2O_4. However, part of the signal arose from the small amount of calcite present in the raw sample (Fig. 6c). At 600–800 °C, calcite and dolomite (from the raw material) disappeared; CaO and MgO were formed (Fig. 6d–f). These results were in agreement with the mechanism proposed by several authors for the thermal decomposition of weddellite and whewellite [20–23]. The decomposition mechanism of weddellite is the following:

$$CaC_2O_4{\cdot}2H_2O \rightarrow CaC_2O_4 + 2H_2O$$

$$CaC_2O_4 \rightarrow CaCO_3 + CO$$

$$CaCO_3 \rightarrow CaO + CO_2$$

Decomposition occurs in three steps. First, water is lost. Carbon monoxide and carbon dioxide are lost in the second and third steps, respectively. No other transformations occur at higher temperatures (Fig. 6e and f).

The thermal analyses (TG, DTA and DTG –differential thermogravimetry–) of a commercial sample of $CaC_2O_4{\cdot}H_2O$ (provided by FLUKA) under air atmosphere are shown in Fig. 7.

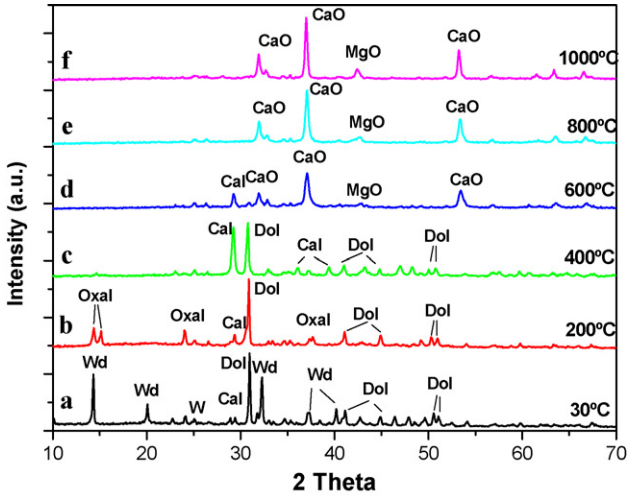

Fig. 6. X-ray diffraction diagrams collected at different temperatures (30, 200, 400, 600, 800 and 1000 °C) [Dol = dolomite, Wd = weddellite, Cal = calcite, W = whewellite, Oxal = calcium oxalate (CaC_2O_4), CaO = calcium oxide, MgO = magnesium oxide].

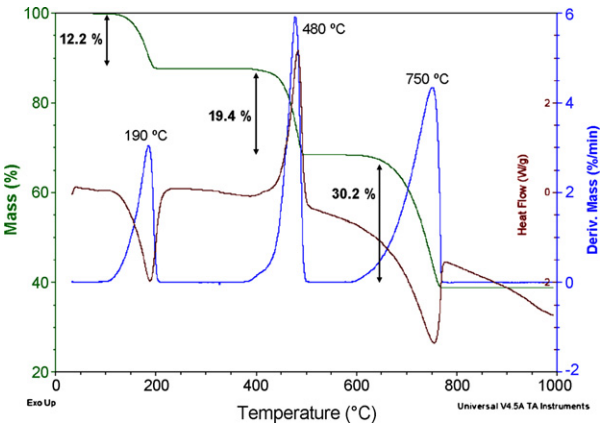

Fig. 7. TG/DTA/DTG curves of a standard sample of whewellite (under air atmosphere).

Table 1
Mass loss percentages during heating of the commercial sample of $CaC_2O_4{\cdot}H_2O$ under air and nitrogen atmospheres.

Temperature range	Around 190 °C (H_2O)	Around 480 °C (CO mainly)	Around 750 °C (CO_2)
Mass loss (air atmosphere Fig. 7)	12.2%	19.4%	30.2%
Mass loss (N_2 atmosphere, figure not shown)	12.7%	18.7%	29.5%

Two endothermic effects (at 190 and 750 °C) and one exothermic effect (at 480 °C) were observed, and these effects corresponded to three mass-loss steps. The thermal study of $CaC_2O_4{\cdot}2H_2O$ (data not shown) revealed similar effects to those described for the monohydrated oxalate, although there were differences in the temperatures at which these effects occurred. Simons and Nerwik [36] showed that the results of the thermal analysis depended on the way in which the experiments are performed. However, Gal et al. [37] showed that the dehydroxylation temperature of synthetic tri-, di- and monohydrates was dependent upon the bonding of water. The results were in agreement with the mechanism proposed by some authors [20–23] and were also in agreement with the DTG curves showed by Frost and Weier [18,21]. The three mass-loss steps were well-defined, and no other effects in the TG/DTG curves were detected between steps. We also perform experiments (TG, DTA and DTG) on the commercial sample of hydrated Ca-oxalate under nitrogen atmosphere (inert). Table 1 shows the percentages of mass losses corresponding to the different effects. Although very similar results were obtained, the percentages which correspond to CO and CO_2 evolving are minor under the inert atmosphere, as expected.

Fig. 8 shows the DTA, TG and DTG curves (experiments performed in air) obtained from patina samples taken from the external monument rocks. The DTA curve showed two endothermic effects and one exothermic effect at temperatures similar to those observed when examining a whewellite standard (Fig. 7). In addition, one exothermic effect appeared; it started at about 155 °C and finished at about 460 °C, with a maximum at about 350 °C. All of these effects were accompanied by mass losses. The percentage of the mass loss that did not occur in the standard sample (between 155 and 460 °C) was higher (16.1%) than the mass loss of water at ~150 °C (about 9.0%) and of CO at 460 °C (about 7.8%) (Fig. 8). The four effects that appeared in the patina samples were not well-defined, contrary to those observed in the standard samples. A continuous mass loss occurred between the different steps.

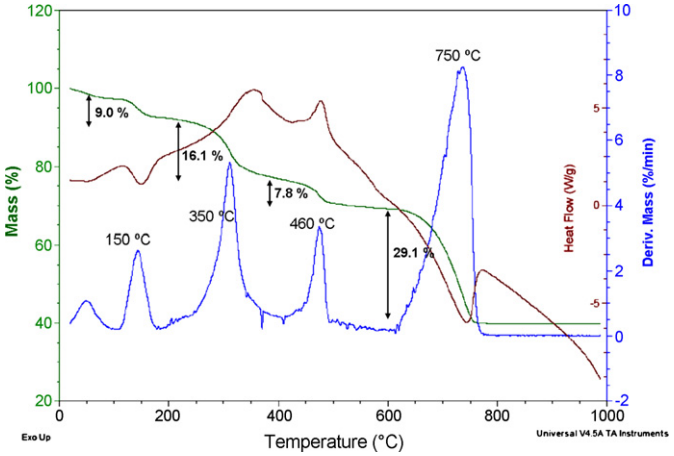

Fig. 8. TG/DTA/DTG curves of a patina sample examined under flowing air.

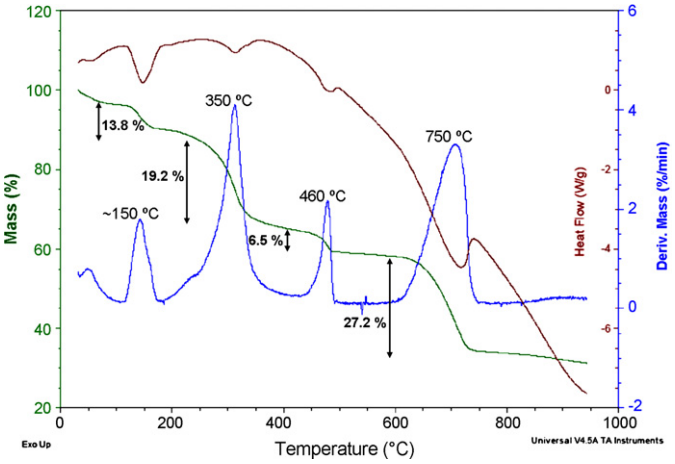

Fig. 9. TG/DTA/DTG curves of a patina sample examined under flowing nitrogen.

These data confirmed that new compounds were present. These compounds were responsible for the new exothermic effect and for the slope of the TG curve. These compounds were not detected by XRD, possibly due to their amorphous character. Fig. 9 shows the results of a thermal study performed on the patina examined in a nitrogen atmosphere. The new exothermic effect that appeared in the thermal study in air between 155 and 460 °C (i.e., combustion) was transformed into an endothermic effect that occurred at about 180–450 °C (i.e., decomposition). These results suggested the presence of organic compounds in the patina. The mass loss in the range 200–400 °C is under nitrogen (inert atmosphere) (19.2%) larger than in air (16.1%) due to the heterogeneity of the samples studied. Other experiments were performed with samples from the Church which were mixed for gaining more homogeneity (figures not shown). The experiments illustrate that the mass loss is larger in air (2.8%) than in nitrogen (2.1%) in this temperature range, as expected by the combustion of the organic residue.

Carbonates show distinctive endothermic peaks at around 840 °C (calcite) and doublets at around 780 °C and at 860 °C (dolomite). Their positions may vary depending on the grain size, the experimental atmosphere and other concomitant factors. The features correspond to the escape of CO_2 during breakdown of mineral's structure. DTA is capable of differentiating high-calcium limestones, dolomites and intermediate materials (e.g., dolomitic limestones). The use of a carbon dioxide atmosphere during heating raises the calcite peak temperature and sharpens it considerably [38–43]. Thermal study of the patina samples, conducted under flowing CO_2 (Fig. 10), revealed two endothermic effects at 780 and 935 °C that corresponded to two mass losses. The first effect (at about 780 °C) exhibited a mass loss of 8.1% and was attributed to the CO_2 loss from magnesium carbonate in the sample's dolomite content. The dolomite originated from the rock substrate. The second effect (at about 935 °C) exhibited a mass loss of 20.6%, which was attributed to the CO_2 produced from the three following processes: the thermal decomposition of the calcium carbonate in the sample's dolomite content, the $CaCO_3$ formed by the thermal decomposition of CaC_2O_4 and the small amount of $CaCO_3$ present in the patina samples from the rock substrate. The mass loss of CO_2 from the magnesium content should be similar to the loss from the calcium content in the dolomite, 8.1%, according to the result from the X-ray diffraction, which exhibited similar values for calcium and magnesium content in the dolomite (1:1). In the XRD analysis, $CaMg(CO_3)_2$ was detected, and there were no other calcium–magnesium carbonates with an intermediate calcium/magnesium ratio. The difference between the total mass loss at 935° C (20.6%) and the total mass lost at 780 °C (8.1%) was

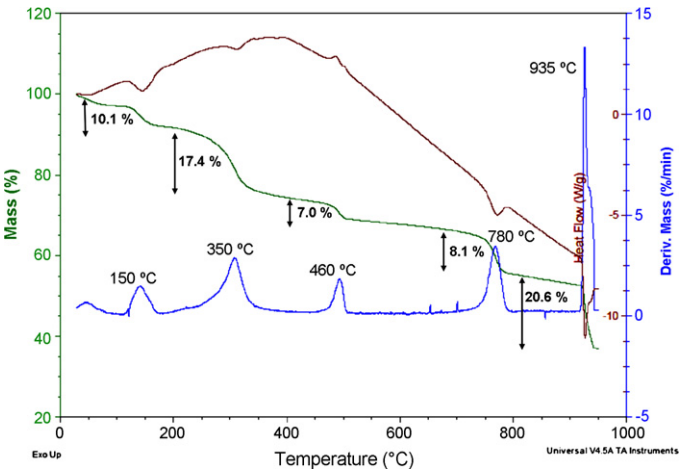

Fig. 10. TG/DTA/DTG curves of a patina sample examined under flowing CO_2.

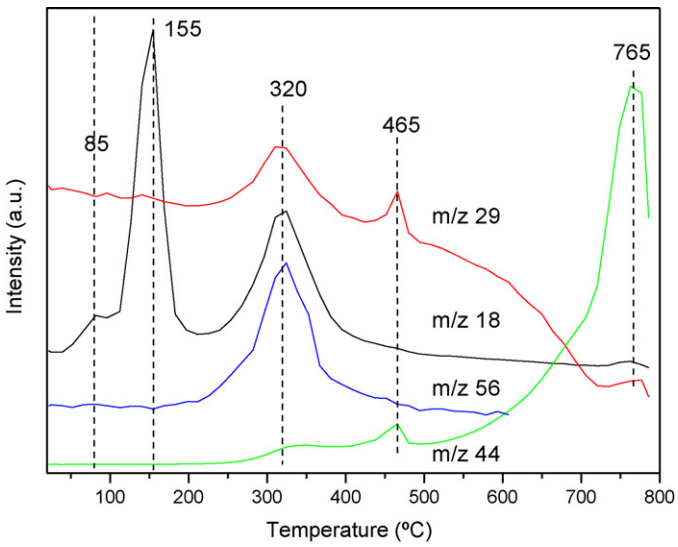

Fig. 11. Mass spectrometry analysis of the gases evolved from the patina samples during the temperature-programmed oxidation under synthetic air (m/z = 44:CO_2, m/z = 29:CO, m/z = 18:H_2O, m/z = 56:representative mass of heavy organic compounds). To clarify the analysis, the intensity has been multiplied by 100 for m/z = 29, by 5 for m/z = 18 and by 500 for m/z = 56.

12.5%, a percentage which corresponded to the CO_2 arising from the $CaCO_3$ formed via decomposition of calcium oxalate (percentages of around 7.0% referred to CO evolving were calculated at 460 °C) and from the low percentage of $CaCO_3$ present in the patina. The percentage of this individual component ($CaCO_3$) was determined from the intensities of the XRD reflections (Figs. 1a and 6a) by the direct method of Cullity and Stock [44]. A value of around 4% was found.

The mass loss between 155 and 460 °C was about 17.4% (Fig. 10), which coincided approximately with the values deduced from Fig. 8 (at around 16.1%). This result confirmed that a high proportion of the organic compounds are present in the patina. Results obtained are different due to the heterogeneity of the samples studied.

Several authors have proposed mechanisms for the formation and evolution of H_2O, CO and CO_2 [20–23]. However, the evolution of CO and CO_2 may bring into question in patina samples constituted by hydrated calcium oxalates that are accompanied by organic compounds. Frost and Weier [18,21] showed that CO_2 is evolved during the second and third mass-loss steps of weddellite/whewellite decomposition. Previously, these losses were only described for the third mass-loss step. Using mass spectrometry, we analysed the gases evolved during thermal treatment of the patina under synthetic air (Fig. 11). The samples were heated at the same rate as that used during the TG measurement (10 °C min^{-1}). Five thermal processes with gaseous product emanation were detected at 85, 155, 320, 465 and 765 °C. These processes corresponded to emanation of water, carbon monoxide, carbon dioxide and other unknown, heavier organic compounds. The temperatures of these processes matched those observed during the thermogravimetric and differential thermal analyses of the patina (Figs. 8–10). In the two lower-temperature processes (85 and 155 °C), only water was evolved. Thus, these events corresponded to the desorption of physically adsorbed water and the crystallisation water of the hydrated calcium oxalates, respectively. At 320 °C, all of the gaseous products were detected. The detected products included water, CO, CO_2 and other gaseous compounds with m/z values up to 68 (in Fig. 11, m/z = 56 was selected as the representative mass value). The simultaneous presence of these compounds suggested that this event corresponded to the combustion and desorption processes of some heavy organic compounds present on the patina. For example, aromatic or aliphatic hydrocarbon compounds with up to five carbon atoms are characterised by ion fragments similar to those observed in our case. Amide or ester compounds could also generate similar fragmentation patterns. Specifically, the m/z = 56 peak could be due to $C_4H_8^+$ or $C_3H_4O^+$ fragment ions, which could proceed from butyl-esters, N-butylamides, pentilcetones, ciclohexenes, tetralines, pentylaromatics and the like. At 465 °C, CO and CO_2 were detected. This observation agreed with the thermogravimetric data, and it was assigned to the decomposition of oxalate to carbonate, a process that produces CO. The detection of CO_2 may be associated with a gas-phase oxidation of the evolved CO by the oxygen in the feed or it may be attributed to the direct evolving of CO_2. Also, the Bouduard reaction can be present; this one implies the CO disproportionation to CO_2 (g) + C (solid). Direct evolution was mentioned by Frost and Weier [18,21], who detected CO_2 during a heating experiment that examined weddellite and whewellite standard samples under a nitrogen atmosphere. Finally, at 765 °C, CO_2 was the primary component, although a small amount of water was also measured. Again, this result was assigned to proposed step for the conversion of calcium carbonate to calcium oxide [20–23]. However, the detection of water suggests the coexistence of a combustion process that was probably acting on the remaining organic species. This process could explain the relative intensity increase of the 765 °C TG peak under an air atmosphere compared to that observed under a nitrogen atmosphere (Figs. 8 and 9). The mass 44 peak, attributed to the occurrence of CO_2, appeared from about 225 °C until about 800 °C, in accordance with the continuous mass loss showed by the slope of the TG curve. The continuous CO_2 gas emanation may be attributed to the continuous decomposition of organic compounds present in the patina samples.

The analysis results for gases evolved from a standard commercial sample of whewellite under synthetic air (Fig. 12a) agreed with the sample's DTA/TG profile (Fig. 7). This agreement confirmed the assignments given to the temperature peaks observed at 155, 465 and 765 °C for the patina sample. At about 495 °C, simultaneous emanation of CO and CO_2 was detected in the standard sample. To verify whether CO_2 was really produced at this temperature (as reported by Frost [18,21]) or if it was generated by the gaseous oxidation of CO by the oxygen atmosphere, a similar study was performed using a helium atmosphere (Fig. 12b). When using helium, the obtained mass profiles were similar to those obtained while using air, but a lower proportion of CO_2 was released at 495 °C. This result suggested that both the direct liberation of CO_2 and the gaseous oxidation of CO occurred at that temperature, but also CO disproportionation is possible.

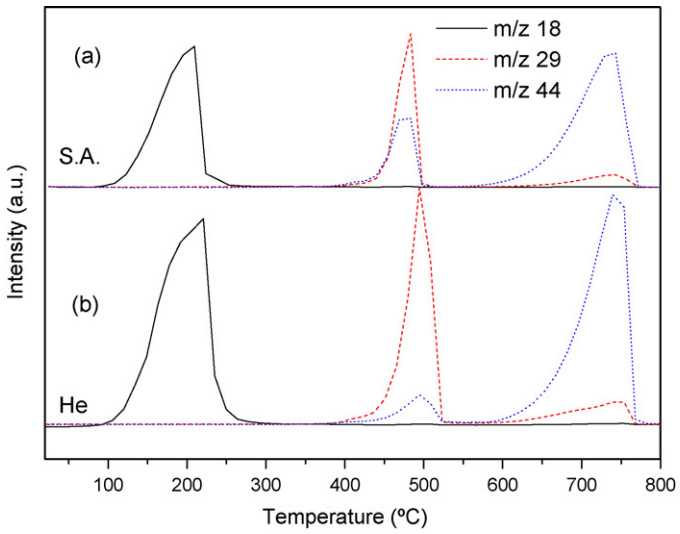

Fig. 12. Mass spectrometry analysis of the gases evolved from a standard commercial sample of whewellite examined under synthetic air (S.A.) (a), and helium (He) (b) atmospheres (m/z = 44:CO_2, m/z = 29:CO, m/z = 18:H_2O).

To better characterise the organic compounds present in the patina, DRIFTS analyses were conducted on the raw patina samples in their original dolomite-rock substrate. A similar analysis was also conducted on a commercial sample of monohydrate oxalate. DRIFTS is a powerful infrared technique that can obtain the IR spectrum of samples in their original from without any treatment, and it is more sensitive to surface species than transmission IR [45]. The obtained spectra were very complex and differed slightly between regions of the sample and between samples due to the heterogeneity of these ones (Fig. 13). Also, a large number of new bands appeared in addition to the bands associated with adsorbed water, carbonates, silicates and oxalates. Although an unambiguous identification of the organic compounds responsible such bands was difficult, signals were obtained for C–H (bands at 3025, 2972, 2936, 2900 and 2876 cm^{-1}) and C=O (bands at 1885, 1815, 1797 and 1738 cm^{-1}) stretching regions. This result suggested the presence of several aliphatic and/or aromatic compounds containing C=O groups; the presence of these compounds agreed with the mass spectrometry detection of m/z = 56 fragment ions ($C_4H_8^+$ or $C_3H_4O^+$) in the gases evolved at 320 °C in air. Only the bands for oxalate and adsorbed water were observed during analysis of the commercial standard.

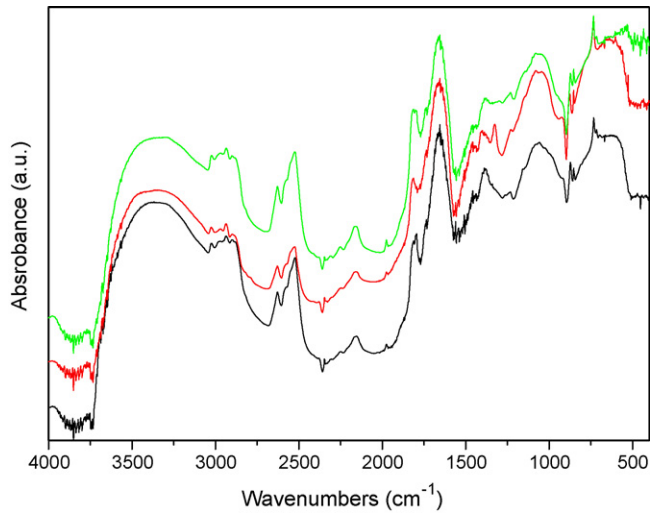

Fig. 13. DRIFT spectra from three regions of the raw patina on its original rock substrate.

4. Conclusions

A multi-analytical combination of techniques was used to study the thermal decomposition of patina formed on Torme's Church. We used DTA, TG and DTG techniques with atmospheres of air, N_2 or CO_2. Further, we also used X-ray diffraction with a high-temperature chamber, SEM-EDX, FT-IR and DRIFTS analyses. Mass spectrometry was used to detect the gases produced at different temperatures.

The room-temperature XRD study revealed the presence of weddellite and a minor amount of whewellite in the patina samples. In addition, dolomite and small amounts of calcite were present; both probably arose from the rock substrate. The oxalate compounds were possibly formed due to microbial degradation of organic products applied for the conservation/restoration of the building. X-ray diffraction analyses were performed at different temperatures (between 30 and 1100 °C). Weddellite and whewellite lost their crystallisation water between 100 and 200 °C and formed calcium oxalate, which transformed into calcium carbonate at 400 °C. This latter compound finally loses CO_2 at 600 °C and becomes calcium oxide. Dolomite and small amounts of calcite, which were also present in the patina samples, were transformed to CaO and MgO at the highest temperature.

The DTA, TG and DTG measurements performed in air revealed thermal effects and mass losses at about 190, 480 and 750 °C; these results confirmed the mechanism deduced using X-ray diffraction. However, a broad exothermic effect (between 155 and 450 °C) appeared in the DTA curve and was associated with an important mass loss. This new effect was attributed to the decomposition of organic compounds present in the patina. The TG and DTA experiments, performed under flowing CO_2, showed the shift of the $CaCO_3$ decomposition to high temperature and its separation from the decomposition of $MgCO_3$ that appeared at lower temperature. We have quantified the amount of some specific components from the patina taking into account the heterogeneity of the samples collected.

The mass spectrometry analyses performed while heating the samples showed the formation of CO_2 from 225 to 800 °C, an effect that was attributed to the continuous decomposition of organic compounds present in the patina. At 320 °C, the simultaneous presence of H_2O, CO, CO_2 and some other compounds with m/z values up to 68 suggested the presence of some heavy organic compounds; this result was in accordance with the TG/DTA results. The increased mass losses at about 465 °C (the temperature of CO formation via decomposition of CaC_2O_4) could be explained by the simultaneous presence of CO_2, which was generated via direct liberation, via CO oxidation or due to the Bouduard reaction.

DRIFTS spectra suggested that several aromatic and/or aliphatic compounds, which contain C=O groups, were present. These results matched well with the mass-spectral detection of m/z = 56 fragment ions. Such fragments could arise from butyl-esters, pentilcetones, ciclohexenes, pentylaromatics, etc.

The analyses performed on a commercial sample of $CaC_2O_4{\cdot}H_2O$ obtained similar results to those described for the patina sample, except that the standard samples exhibited none of the effects derived from the presence of organic compounds.

Acknowledgements

The authors gratefully acknowledge Dr. M.C. Jimenez de Haro for her assistance and the financial support from project BIA 2009-12618 and contract JAEDoc 088.

References

[1] E. Diakumaku, A.A. Gorbushina, W.E. Krumbein, L. Panina, Sci. Total Environ. 167 (1995) 295.
[2] U. Wollenzien, G.S. de Hog, W.E. Krumbein, C. Urzi, Sci. Total Environ. 167 (1995) 287.
[3] M. García-Vallés, C. Urzi, F. De Leo, P. Salamone, M. Vendrell-Saz, Int. Biodeterior. Biodegrad. 46 (2000) 221.
[4] M. del Monte, C. Sabioni, Environ. Sci. Technol. 17 (1983) 516.
[5] M. del Monte, C. Sabbioni, G. Zappia, Sci. Total Environ. 67 (1987) 17.
[6] J. Chen, H.P. Blume, L. Beyer, Catena 39 (2000) 121.
[7] H.G.M. Edwards, N.C. Russell, M.R.D. Seaward, Spectrochim. Acta Part A 53 (1997) 99.
[8] L. Lazzarini, E. Borrelli, M. Bouabdelli, F. Antonelli, J. Cult. Herit. 8 (2007) 315.
[9] L. Lazzarini, O. Salvatori, Stud. Conserv. 34 (1989) 20.
[10] B. Prieto, M.R.D. Seaward, H.G.M. Edwards, T. Rivas, B. Silva, Biospectroscopy 5 (1999) 53.
[11] J.V. Liebigs, Ann. Chem. Pharm. LXXXVI (1953) 113.
[12] B.D. Mitchell, A.C. Birnie, J.K. Syers, Analyst 91 (1966) 783.
[13] K.P. Pribylov, D.S. Fazlullina, Zh. Neorg. Khim. 14 (1969) 660.
[14] B. Tomazic, G.H. Nancollas, J. Cryst. Growth 46 (1980) 355.
[15] P. Giordani, P. Modenesi, M. Tretiach, Lichenologist 35 (2003) 255.
[16] I. Martinez-Arkarazo, D.C. Smith, O. Zuloaga, M.A. Olazabal, J.M. Madariaga, J. Raman Spectrosc. 39 (2008) 1018.
[17] K. Kolo, Ph. Claeys, Biogeosciences 2 (2005) 277.
[18] R.L. Frost, M.L. Weier, Thermochim. Acta 406 (2003) 221.
[19] L. Campanella, E. Cardarelli, R. Curini, G. D'ascenzo, M. Tomasetti, J. Therm. Anal. Calorim. 38 (1992) 2707.
[20] F. Carrasco, Afinidad 48 (1991) 19.
[21] R.L. Frost, M.L. Weier, Thermochim. Acta 409 (2004) 79.
[22] S. Gurrieri, G. Siracusa, R. Cali, J. Therm. Anal. Calorim. 6 (1974) 293.
[23] J. Mu, D.D. Perlmutter, Thermochim. Acta 44 (1981) 207.
[24] A. Duran, M.D. Robador, J.L. Perez-Rodriguez, Study of the degradation processes happening on two historical buildings from Northern Spain by formation of oxalate and sulphate-based compounds, Internat. J. Architec. Herit., submitted for publication.
[25] T. Echigo, M. Kimata, A. Kyono, M. Shimizu, T. Hatta, Mineral. Mag. 69 (2005) 77.
[26] M. Aulinas, M. Garcia-Valles, D. Gimeno, J.L. Fernandez-Teruel, F. Ruggieri, M. Puges, Environ. Sci. Pollut. Res. 16 (2009) 443.
[27] A. Bralia, M. Matteini, A. Moles, G. Sabatini, Proceedings of the 1st International Symposium "The oxalate films", Centro Gino Bozza, Milan, 1989, pp. 75–84.
[28] P.V. Monje, E.J. Baran, Plant Physiol. 128 (2004) 707.
[29] F. Lebisque, J. Rech. Nat. Sci. Lab. Bellaire 14 (1963) 33.
[30] F. Cariati, R. Rampazzi, L. Toniolo, A. Pozzi, Stud. Conserv. 45 (2000) 180.
[31] H.T. Horner, L.H. Tiffani, G. Knaphus, Mycologie 87 (1995) 34.
[32] E.P. Verrechia, J.L. Dumont, K.E. Verrechia, J. Sed. Geol. 63 (1993) 1000.
[33] E.P. Verrechia, in: R.E. Riding, S.M. Awranik (Eds.), Microbial Sediments, Springer Verlag, Berlin, Heidelberg, New York, 2000, pp. 68–75.
[34] G.M. Gadd, Adv. Microb. Physiol. 41 (1999) 47.
[35] S.L. Jackson, I.B. Heath, Microbiol. Mol. Biol. Rev. 57 (1993) 367.
[36] E.L. Simons, A.E. Nerwik, Talanta 11 (1964) 549.
[37] S. Gal, F. Paulik, L. Erdey, J. Bayer, Period. Polytech. 7 (1963) 215.
[38] A. Moropoulou, A. Bakolas, K. Bisbikou, J. Cult. Herit. 1 (2000) 45.
[39] C. Genestar, C. Pons, A. Mas, Anal. Chim. Acta 557 (2006) 373.
[40] T.L. Webb, J.E. Kruger, in: R. Mackenzie (Ed.), Differential Thermal Analysis, Academic Press, London, 1970, pp. 303–341.
[41] V. Vágvölgy, R.L. Frost, M. Hales, A. Locke, J. Kristof, E. Horváth, J. Therm. Anal. Calorim. 92 (2008) 893.
[42] C.W. Beck, Am. Mineral. 35 (1950) 985.
[43] A. Duran, L.A. Perez-Maqueda, J. Poyato, J.L. Perez-Rodriguez, J. Therm. Anal. Calorim. 99 (2010) 803.
[44] B.D. Cullity, S.R. Stock, Elements of X-ray Diffraction, Addison-Wesley Publishing Company, Reading, MA, USA, 2001.
[45] M.A. Centeno, J.J. Benitez, P. Malet, I. Carrizosa, J.A. Odriozola, Appl. Spectrosc. 51 (1997) 416.